SENCKENBERG

ORIGINAL PAPER

Shell-specific differentiation: how geometric morphometrics can add to knowledge of Macominae species (Tellinidae, Bivalvia)

Thais Aparecida Marinho[1,2] (ID) · **Eliane Pintor Arruda**[2] (ID)

Abstract

Tellinidae is one of the most diverse families in Brazilian coastal areas, comprising nine subfamilies, one of which is Macominae. These species are known for their morphological similarities, which make their identification difficult. To minimize such difficulties, taxonomists have sought methods or tools, such as the use of geometric morphometric data, to study the continuous characteristics which are often observed subjectively and are not measurable. Almost thirty right valves were chosen from five of the most representative Macominae species: *Austromacoma biota* Arruda & Domaneschi, 2005, *Austromacoma constricta* (Bruguière, 1792), *Psammotreta brevifrons* (Say, 1834 in Say 1830–1834), *Psammotreta cleryana* (d' Orbigny, 1846 in d' Orbigny 1834–1847), Macoploma tenta (Say, 1834 in Say 1830–1834). The geometric morphometric data were based on the fourteen landmarks of each internal valve, performed by TPSDig, and the morphometric and statistical analyses, carried out with MorphoJ, were Procrustes analysis, Procrustes Anova, principal components analysis, discriminant function analysis, and regression analysis. Permutations and Goodall's F test with bootstrap were performed in the R software package. All the analyses divided the studied species into two groups based on the external shape of their shells: oval-trigonal or elongated. The variation of the external shape of the shell is related to the life habits of the bivalve, with the elongated shells lying inclined in the substrata, and the oval-trigonal shells lying horizontally, facilitating deposit-feeding habits. The pallial sinus shape and position of the adductor muscle scar also helped differentiate species of each group, relating them to the bivalve anatomy. *Psammotreta cleryana* and *P. brevifrons* exhibited remarkably similar shapes, and a broader population study is needed to differentiate between these two species.

Keywords Mollusca · Morphology · Taxonomy · *Austromacoma* · *Psammotreta* · *Macoploma*

Introduction

Tellinidae is one of the most diverse families found in the Brazilian continental shelf. Huber (2015) recognizes nine subfamilies of Tellinidae: Tellininae, Gastraninae, Phyllodainae, Moerellinae, Aenigmotellinae, Arcopaginae, Apolymetiinae, Strigillinae, and Macominae. Macominae is characterized by rounded, inequilateral shells, with strong to weak hinges,

containing two cardinal teeth, being one bifid, and lateral teeth absent. The sculpture is mostly commarginal and weak, and the periostracum is usually strong. The adductor muscle scars are subequal, and there is a deep pallial sinus (Mikkelsen and Bieler 2008; Huber 2015). Macominae includes seventeen living genera divided into five groups (Huber 2015): *Psammotreta*, *Salmacoma*, *Psammacoma*, *Austromacoma*, and *Macoma*. On the Brazilian coast, six species have been registered to these groups: *Austromacoma biota* Arruda & Domaneschi, 2005, *Austromacoma constricta* (Bruguière, 1792), *Psammotreta cleryana* (d' Orbigny, 1846 in d' Orbigny 1834–1847), *Psammotreta brevifrons* (Say, 1834 in Say 1830–1834), *Macoploma tenta* (Say, 1834 in Say 1830–1834), and *M. tageliformis* (Dall, 1900) (Rios 2009). The separation of Macominae from the other subfamilies based only on the absence of lateral teeth has been considered a mistake, and the subfamily has been considered paraphyletic (Huber 2015) and even polyphyletic (Coan and Valentich-Scott 2012).

✉ Eliane Pintor Arruda
arruda@ufscar.br

1 Programa de Pós-Graduação em Biologia Animal, Instituto de Biologia, Universidade Estadual de Campinas, Campinas, SP, Brasil

2 Laboratório de Estudos em Macroinvertebrados Bentônicos, Departamento de Biologia, Centro de Ciências Humanas e Biológicas, Universidade Federal de São Carlos, campus Sorocaba, Sorocaba, SP, Brasil

There is little information about Macominae species from the Western Atlantic, except for the surveys carried out by Tenório et al. (1986), Narchi (2003), Arruda and Domaneschi (2005), Piffer et al. (2011), and Huber (2015). The identification of Macominae and other Tellinidae species are based on shell morphology, which have diverse and homoplastic characteristics (Simone and Wilkinson 2008; Huber 2015). Despite the many limitations of using shell morphological data for taxonomy, the method remains widely used due to the need to identify through observable characters.

Therefore, taxonomists have sought different methods and tools to help them minimize difficulties with identification, one of which is morphometric analysis. This method provides statistical support to identify differences in continuous characteristics, which are often observed subjectively and not measurable. For example, Marko and Jackson (2001) studied the shell morphometry of five pairs of cryptic bivalve species of *Arcidae* separated by the Isthmus of Panama, while Rufino et al. (2006) separated two commercially fished Venus clams (Veneridae family) using both contour- and landmark-based methods. Since Bookstein (1991), the geometric morphometric method has been used as a tool to quantify the morphological modifications of an organism throughout its evolution processes. Unlike linear morphometry, the geometric morphometric approach separates shape and size and represents deformations through graphical structures (Bookstein 1991; Rohlf and Marcus 1993; Reis 1998; Rohlf 2000a, b, c; Jensen 2003; Moraes 2003; Adams et al. 2004; Sheets et al. 2006; Rocha 2011). Although this methodology has not been explored as much as other approaches in the study of mollusks, some studies have demonstrated that it may be applied for different purposes (Anderson 2001; Anderson and Roopnarine 2005; Inoue et al. 2014; Kosnik et al. 2006; Marquez et al. 2017; Monnet et al. 2009; Vuolo et al. 2011).

Therefore, the goal of is the present study was to identify morphometric characters using *Psammotreta*, *Austromacoma*, and *Macoploma* species shells, in order to improve taxonomic identification and increase knowledge of the life habits of Tellinidae.

Materials and methods

Samples from the Zoology Museum of the Sao Paulo University (MZUSP) and the Adão José Cardoso Zoology Museum of the State University of Campinas (ZUEC) were reviewed and underwent species recognition, following which five species, which were well represented in a number of individuals, were selected. Approximately thirty adults of each of the following species were selected—*Austromacoma biota*, 26; *A. constricta*, 28; *Psammotreta brevifrons*, 11; *P. cleryana*, 26; and *Macoploma tenta*, 28 (Fig. 1).

Fig. 1 Macominae species studied. **a–b** *Austromacoma biota* (Arruda & Domaneschi, 2005); **a** internal surface ZUEC-BIV 2192, Cidade Beach, Caraguatatuba Municipality SP; **b** external surface, holotype MZUSP 41183, Cidade Beach, Caraguatatuba Municipality, SP; **c–d** *Psammotreta brevifrons* (Say, 1834 in Say 1830–1834) MZUSP 21974, Ubatuba Municipality, SP; **c** internal surface; **d** external surface; **e–f** *Austromacoma constricta* (Bruguière, 1792), UFScar Collection, Araçá Bay, São Sebastião Municipality, SP; **e** internal surface; **f** external surface; **g–f** *Psammotreta cleryana* (d'Orbigny, 1846 in d'Orbigny 1834–1847) MZUSP 43893, Bertioga Municipality, SP; **g** internal surface; **h** external surface; **i–j** *Macoploma tenta* (Say, 1834 in Say 1830–1834) MZUSP 21949, Andorinhas Beach, Ubatuba Municipality, SP; **i** internal surface; **j** external surface

Fourteen (14) landmarks were selected using the internal region of the right valve for each individual (Fig. 2). The internal region was chosen due to having the most similar points among the species, including the intersection of the muscle scars and the extreme points of the shell curvature. Using the Bookstein (1991) classification of landmarks as type one, two, and three, those selected were classed as follows: landmarks 1, 3, 4, and 5 were type one; landmarks 2, 6, 7, 9, and 10 were type two; and landmarks 8, 11, 12, 13, and 14 were type three (Fig. 2). The images were taken by a 12.1 megapixel Canon Power Shot SX50 HS58 digital camera fixed to a tripod and from the same distance for all the valves.

The x- and y-coordinates of each landmark were obtained using the TpsDig software package, version 2.30 (Rohlf et al. 2004), and general Procrustes analysis (GPA) was used to quantify shape and size variation. This analysis applies a least-square superposition algorithm to a set of Cartesian coordinates of anatomical landmark configurations, which broadly represent the shape of the specimen (Rohlf 1990). This procedure fits each configuration to the mean shape of the sample as closely as possible, so that size, position, and orientation remain constant according to the criterion for the least-squares fit. Consequently, the remaining variation in landmark positions is due to the variation of shape (Klingenberg 2013).

The GPA, in addition to most statistical analyses, were carried out using the MorphoJ software package, version 1.06d, which provides a user-friendly platform for a broad range of morphometric analyses (Klingenberg 2011). MorphoJ uses a full Procrustes fit and projects the data to the tangent linear Euclidean space by orthogonal projection, which produces a new set of shape variables, a variation/covariation matrix of shape coordinates (Klingenberg 2011), which were used in multivariate statistical analyses. The point of tangency between the two spaces, the Procrustes shape space and the Euclidean space, is the mean or consensus shape of the sample (Viscosi and Cardini 2011).

The relative displacement from one average configuration to another, or from one shape to another in the shape space, can be used to analyze the differences between shapes (Klingenberg 2013). Thus, shape changes were described
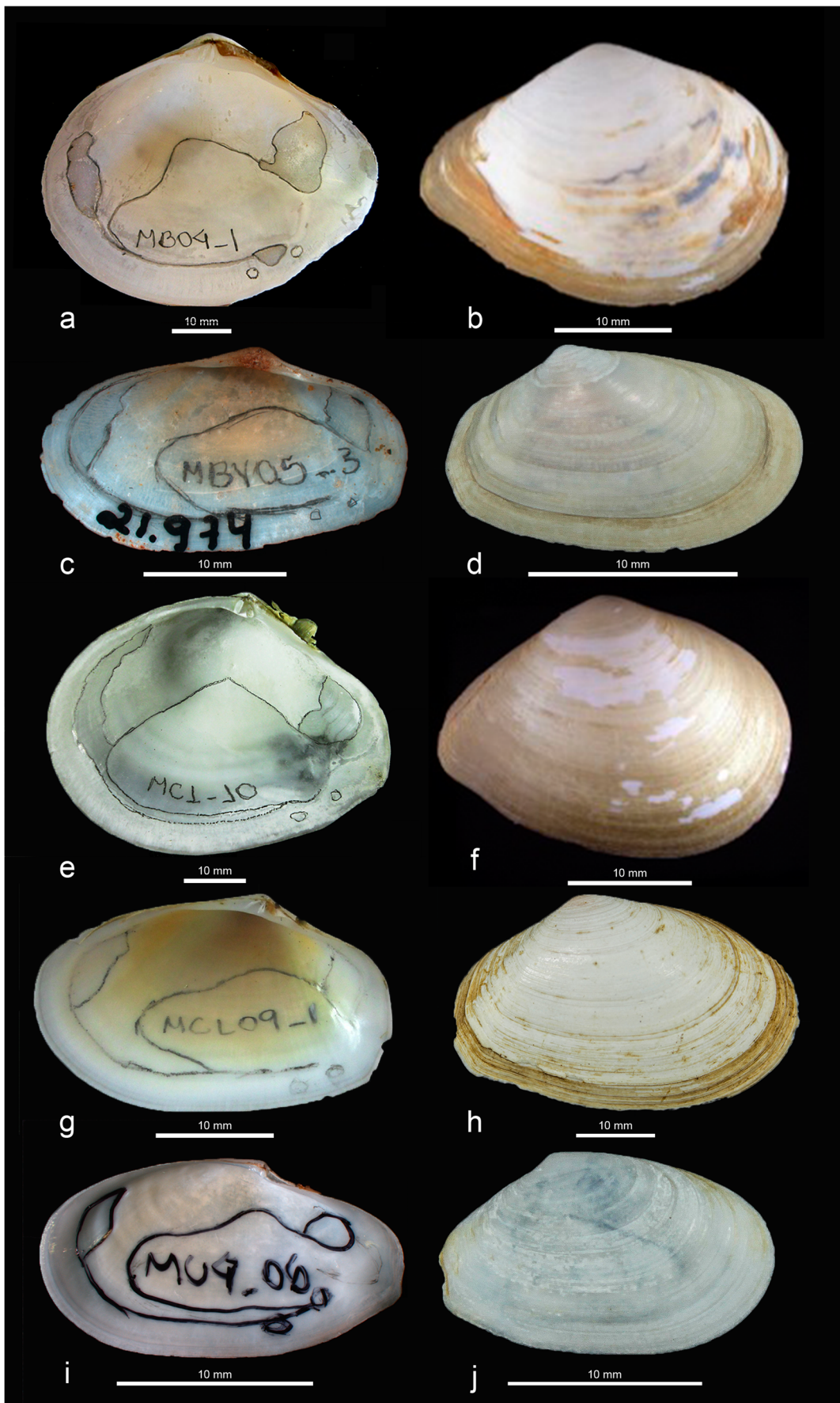
Fig. 2 Landmark or homologous points configuration. Landmarks: 1, extreme dorsal point; 2, beak of umbo; 3, extreme anterior point; 4, extreme ventral point; 5, extreme posterior point; 6, extreme ventral point of posterior muscle scar; 7, extreme dorsal point of posterior muscle scar; 8, intersection between pallial sinus and posterior muscle scar; 9, extreme dorsal point of pallial sinus; 10, extreme anterior point of pallial sinus; 11, intersection between pallial sinus and pallial line; 12, intersection between pallial line and anterior muscle scar; 13, anterior cruciform muscle scar; and 14, posterior cruciform muscle scar
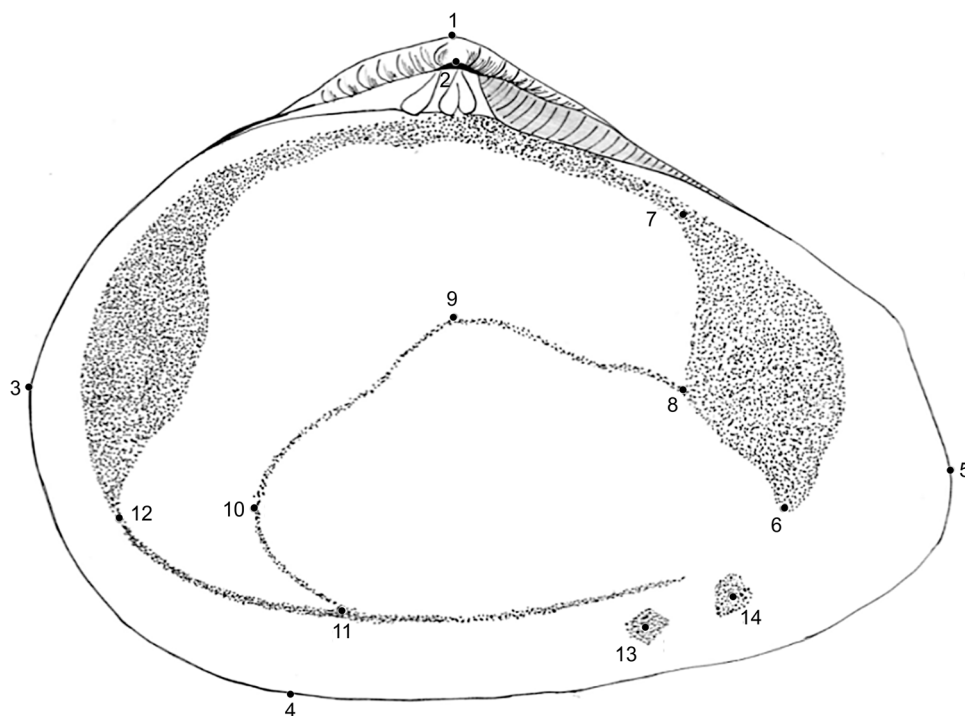
using two wireframes based on landmark displacement: one for the starting shape, usually a consensus, and another for the target shape to be analyzed.

Procrustes Anova was used to assess the relative amount of variation among species. However, as MorphoJ does not allow permutation procedures, it was also performed in R software, using the geomorph package (Adams et al. 2021). For this, the matrix with the Cartesian coordinates of the landmarks was exported from MorphoJ, and GPA was performed again in R software, providing the variation matrix of GPA shape coordinates used in Procrustes Anova. Principal components analysis (PCA) was carried out to identify and account for the redundancy of the variation/covariation matrix of the GPA shape coordinates. In addition, PCA displays the major shape variation features. Finally, to test the separation of shell shapes between the Macominae species, linear discriminant analysis (LDA) using the leave-one-out cross-validation procedure was performed to estimate the reliability of the discrimination. In such validation, an individual is left out of the analysis, one-by-one, and prediction is performed using data from all the other specimens. In this way, the cross-validation predictions avoid "circular reasoning," where a specimen is classified using functions calculated with samples that included the specimen itself. MorphoJ automatically includes a parametric *T-square* test for the difference between group means in LDA and provides both Procrustes distance and the Mahalanobis distance, comparing the shape of species pair by pair. The LDA performed in MorphoJ considers the dataset to be parametric. As the data only seldom comply with all the assumptions of the parametric tests, the species were

compared pair by pair using Goodall's *F* test with bootstrap in R software, using the shapes' package (Dryden 2019), and the results obtained from the LDA and Goodall's *F* test were compared. Two other permutation tests with the same objective of comparing the shape of the species pair by pair were also performed, the Hotelling test with permutations in the R software (Dryden 2019) and two groups with permutations in the Past software (Hammer et al. 2001). The results of these tests are available in the supplementary material.

To study the relationship between the variation of geometric shape and size of individuals from the Macominae species, a multivariate regression of the Procrustes coordinates onto a measure of size was used. For each independent variable, MorphoJ computes a shape score by projecting the shape data onto a line in the direction of the regression vector. According to Drake and Klingenberg (2008), this score is the shape variable associated with the shape changes predicted by the regression model and includes the residual variation in the direction of the shape space. The centroid size was used as a dependent variable. Centroid size is the most used size measure in the geometric morphometric method; it is the square root of the sum of squared distances of all the landmarks of an object from their centroid (Klingenberg 2016). Therefore, regression plot scores versus centroid size can give a visual impression how closely the data point fits a straight line (Klingenberg 2016).

The vector graphics and wireframes were generated by MorphoJ, and the artwork was created using Photoshop version CS6. Further details of these methods are described

extensively in Bookstein (1991), Monteiro and Reis (1999), Zelditch et al. (2004), Viscosi and Cardini (2011), and Klingenberg (2011, 2013, 2016).

Results

As the number of individuals of *P. brevifrons* is much smaller than the other species studied, we initially performed a morphometric analysis without this species and then included it to compare the results. Procrustes Anova analysis indicated significant differences among species in both analyses with and without *P. brevifrons* (Table 1). The analysis carried out with permutations indicated the same results (Table 1).

The graphical representations of principal components analysis (PCA) with and without *P. brevifrons* show differentiations, based, mostly, on the first two axes (Figs. 3 and 4). In PCA analysis without *P. brevifrons*, axis 1 explains 58.7% of the variation and axis 2 16.5% of the variation (Fig. 3), while in PCA with *P. brevifrons*, axis 1 is responsible for 56.2% of the variation, axis 2 for 18.0%, and axis 3 for 7.68% (Figs. 4 and 5). As there were no differences between the initial analyses with and without *P. brevifrons*, only results obtained with *P. brevifrons* will be provided below.

When comparing the consensus with the individual settings in the PCA extreme position, it was observed that axis 1 (Figs. 4 and 5) demonstrates variation on the pallial sinus, specifically in the position of landmark 11, separating *Austromacoma biota* from the other species. In this species, landmark 11 is in a much more anterior position, compared to the consensus shape. Consequently, the pallial sinus is only slightly detached from the pallial line in this species, while in *A. constricta* and *M. tenta*, the pallial sinus is notably detached from the pallial line. *Austromacoma biota* also differs from all the other species through variation in landmarks 13 and 14, which is positioned more posteriorly than the consensus. Axis 2 separates the species into two different groups based on the external shape of their shells. The first group, situated at the most positive end of axis 2, contains three species with elongated shells— *P. brevifrons*, *P. cleryana*, and *M. tenta*, while the second group, situated at the most negative end, contains two species with an oval shell shape—*A. biota* and *A. constricta*. The

variation in the external shape of the shell occurs mainly due to variations in landmarks 1, 3, 4, and 5. On the positive side of axis 2, landmark 1 tends to be in a more ventral position, landmark 3 in a more anterior position, and landmark 4 in a more dorsal and anterior position, causing the species to have a lower and more elongated shape, compared to the consensus shape. On the negative side of axis 2, landmark 1 tends to be more dorsal, landmarks 3 to 4 are almost in the same position as the consensus shape, and landmark 5 is more posterior; consequently, the shells of *A. biota* and *A. constricta* are taller and have an oval shape. Axis 3 (Fig. 5) also exhibited variation on the pallial sinus and the anterior adductor muscle, due to changes in landmarks 10 and 12, respectively. On the positive side of axis 3, landmark 10 tends to be more posterior, so that the pallial sinus is shallower, while landmark 12 tends to be more ventral and posterior, meaning that the posterior adductor muscle has a more ventral-posterior position. On the negative side of axis 3, meanwhile, landmark 10 tends to be more anterior, and consequently the pallial sinus is deeper, while landmark 12 tends to be more dorsal and anterior, so that the anterior adductor muscle has a more dorsal-anterior position. Thus, *A. biota* and *M. tenta* tend to have a deeper pallial sinus and anterior adductor muscle more dorsal than the other species.

The pair-by-pair analysis of the shell shape agreed with the PCA, separating the species into two groups according to the external shape of their shells. Mahalanobis distance compares the species by showing the distance among them, so, in Table 2, the greatest distance was between the oval and elongated shells, supported by the distances between *A. biota* and *P. brevifrons* (32.31), *A. constricta* and *P. cleryana* (22.19), *A. constricta* and *P. brevifrons* (21.88), and *A. biota* and *P. cleryana* (21.49), with *A. biota* and *A. constricta* having the same external shell shape, as well as *P. cleryana* and *P. brevifrons*. The shortest distance was between species with the same shell shape, *P. brevifrons* and *P. cleryana* (5.10), *P. brevifrons* and *M. tenta* (7.97), *P. cleryana* and *M. tenta* (8.13), and *A. constricta* and *A. biota* (11.67). Procrustes distance and the Goodall's *F* test also provided similar results but also showed a great difference between *A. biota* and *M. tenta* and *A. biota* and *A. constricta*, which, despite having the same external shell shape, are quite different in pallial sinus shape and in the position of the anterior adductor muscle (Table 2).

Table 1 Procrustes Anova performed for differences in shape with and without *P. brevifrons* and with and without permutations

		SS	MS	df	*F*	*P*
Without *P. brevifrons*		3.0625	0.03190	96	58.37	<0.0001
	Permutations*	3.0717	1.02389	3	58.571	0.001
With *P. brevifrons*		3.0625	0.00319	96	47.89	<0.0001
	Permutations*	3.2406	0.81015	4	48.091	0.001

SS sum of squares, *MS* mean sum of squares, *df* degrees of freedom

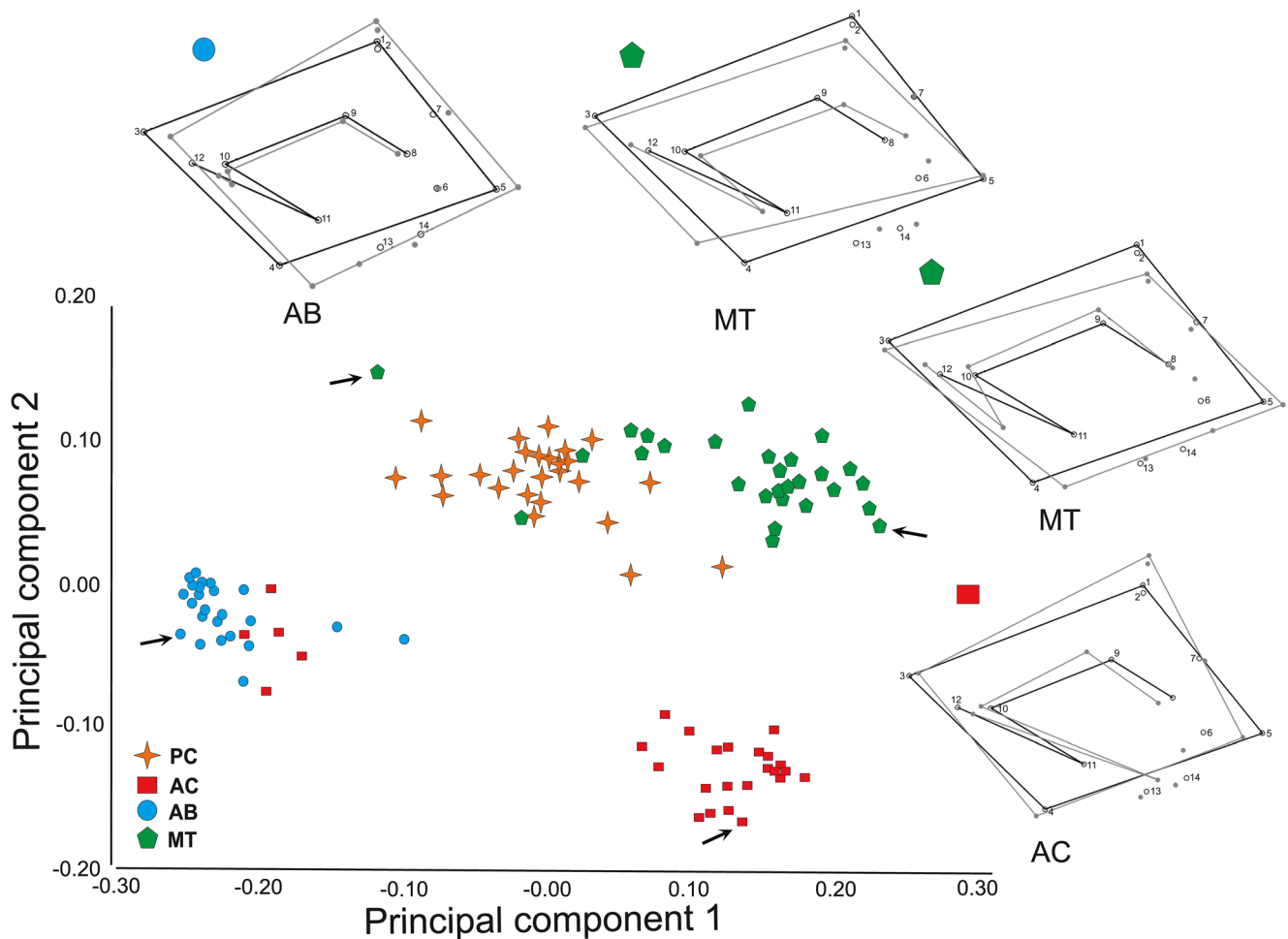*Randomizations of null model residuals/1000 permutations

Fig. 3 Graphical representation of the first and second principal component axes without *Psammotreta brevifrons* in analysis. The wireframes of four specimens (in gray) in extreme positions of the axes compared to the consensus shape (in black) are illustrated to show variation along the first and second principal components axes. The arrows indicate the specimens represented. AB, *Austromacoma biota*; AC, *Austromacoma constricta*; PC, *Psammotreta cleryana*; MT, *Macoploma tenta*

The results obtained with the Hotelling and two groups test with permutations were similar to the Goodall's *F* statistic (supplementary material).

Table 3 presents the cross-validation matrix classification of linear discriminant analysis, with comparison between group 1 and 2 above the diagonal line and comparison of group 2 and group 1 below it. Most species were identified 100% correctly, except for *P. brevifrons*, *P. cleryana*, and *M. tenta*, with the lowest percentage between *P. cleryana* and *P. brevifrons* (72.73%), *P. brevifrons* and *P. cleryana* (73.07%), and *M. tenta* and *P. brevifrons* (78.60%).

The LDA cross-validation scores (Fig. 6) of *P. brevifrons* and *P. cleryana* revealed many overlapped individuals. Compared to the consensus wireframes of these two species, the main difference is between landmarks 3 and 12, with landmark 3 in *P. brevifrons* (black line) dorsally dislocated and landmark 12 ventrally dislocated. The scores of *M. tenta* with *P. brevifrons*

and *M. tenta* with *P. cleryana* are shown in Figs. 7 and 8, respectively. Besides landmarks 10, 11, and 12 previously mentioned, *M. tenta* (gray line) also differs from *P. brevifrons* (black line, Fig. 7) and *P. cleryana* (black line, Fig. 8) in landmark 1, positioned more ventrally, landmark 3, more anteriorly, landmark 5, more posteriorly, landmark 6 more anteriorly and dorsally, landmark 7 more anteriorly and ventrally, and landmarks 8 and 9, positioned more anteriorly, so that *M. tenta* has a more elongated shape and lower posterior adductor muscle than *P. brevifrons* and *P. cleryana*, in addition to a deeper pallial sinus.

Regression analysis did not reveal a clear relationship between shape and size but did show that the elongated shells tend to have smaller centroid sizes than oval shells (Fig. 9). Procrustes Anova analysis confirmed that there was a significant difference between the centroid size of species (*F*= 349.32 and *p* < 0.0001). However,
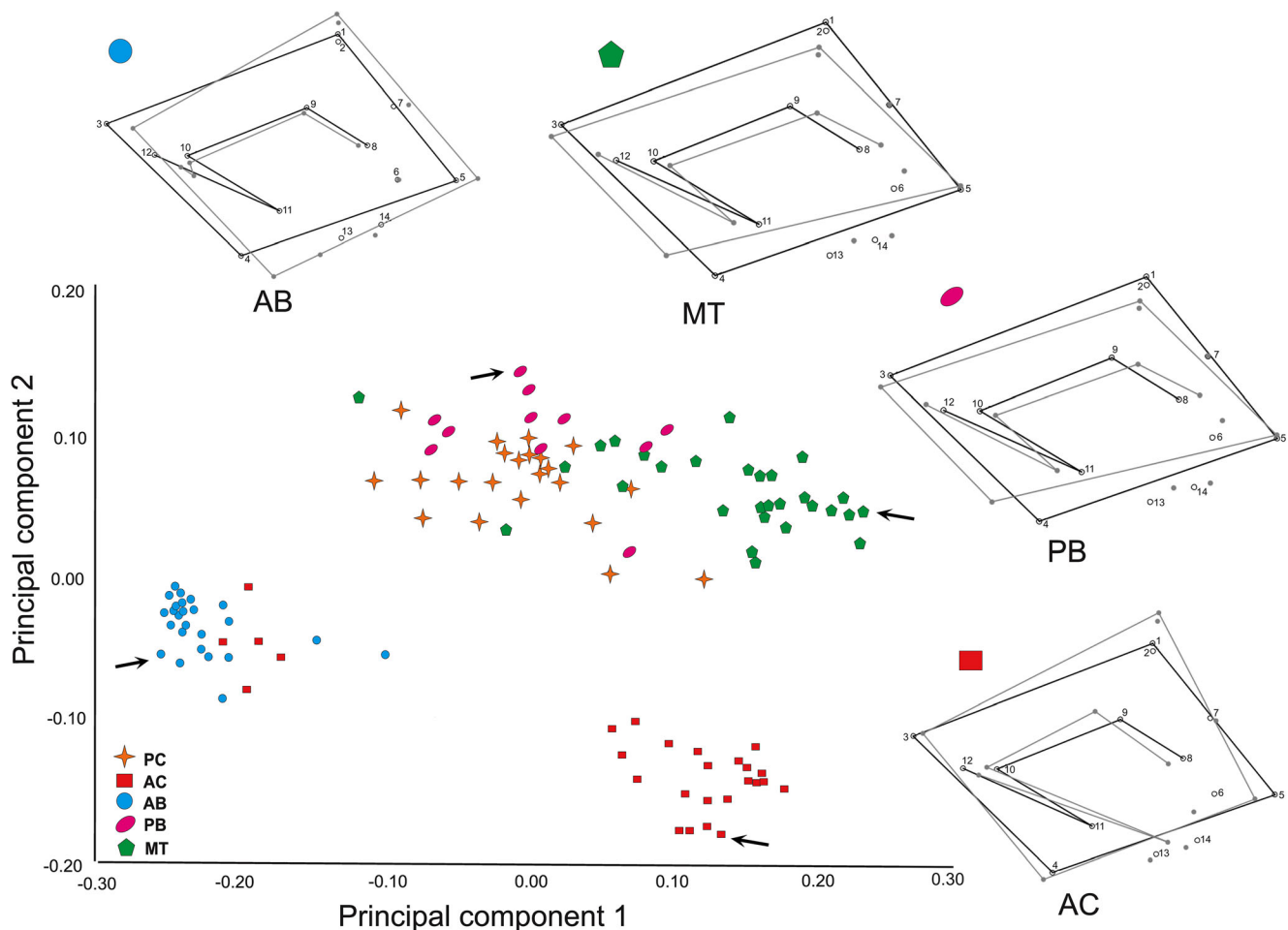
Fig. 4 Graphical representation of the first and second principal components axes including *Psammotreta brevifrons* in analysis. The wireframes of four specimens (in gray) in extreme positions of the axes compared to the consensus shape (in black) are illustrated to show variation along the first and second principal components axes. The arrows indicate the specimens represented. AB, *Austromacoma biota*; PB, *Psammotreta brevifrons*; AC, *Austromacoma constricta*; PC, *Psammotreta cleryana*; MT, *Macoploma tenta*

this result should be considered carefully, as the individuals used in the present study have a restricted size range (Table 4). Table 4 summarizes the information on the shape and size of each species, associating it with information on their life habits.

Discussion

Macominae species have shells with a similar external shape, making their identification by taxonomists difficult (Arruda and Domaneschi 2005; Piffer et al. 2011). The results obtained in the present study identify three main characters that allow differentiation of the analyzed species, supported by geometric morphometric data: the external shape of the shell, the shape of the pallial sinus, and the position of the adductor muscle scars.

The landmarks that identify the differences in the external shape of the shell are 1, 3, 4, and 5, points which allow the separation of the studied species into two groups, oval-trigonal (*A. biota* and *A. constricta*) and elongated shells (*P. cleryana*, *P. brevifrons*, and *M. tenta*). These landmarks were chosen as the most extreme points in the shell where variations mark a change in the external shape and consequently life habits. The Tellinoidea superfamily is known for its infaunal burrow specialists, for which elongated shells are a benefit due to their elongated and streamlined outline, which is generally unsculptured, as well as their extensive siphons and pronounced pallial sinus and central umbo (Watters 1993). Some species lie on the left valve with the long axes horizontal, while others lie with their long axes at angles of up to 30° or 45° (Stanley 1970). Horizontal, or close to horizontal, positioning can offer an advantage to siphonate deposit feeders, facilitating horizontal migrations for better substrate exploitation (Stanley 1970). In the case of the studied species, *A. biota* and *A. constricta* lie horizontally, with prominent posterior curvature to the right, showing that siphons emerge perpendicular to the orientation of the shell (Arruda et al.
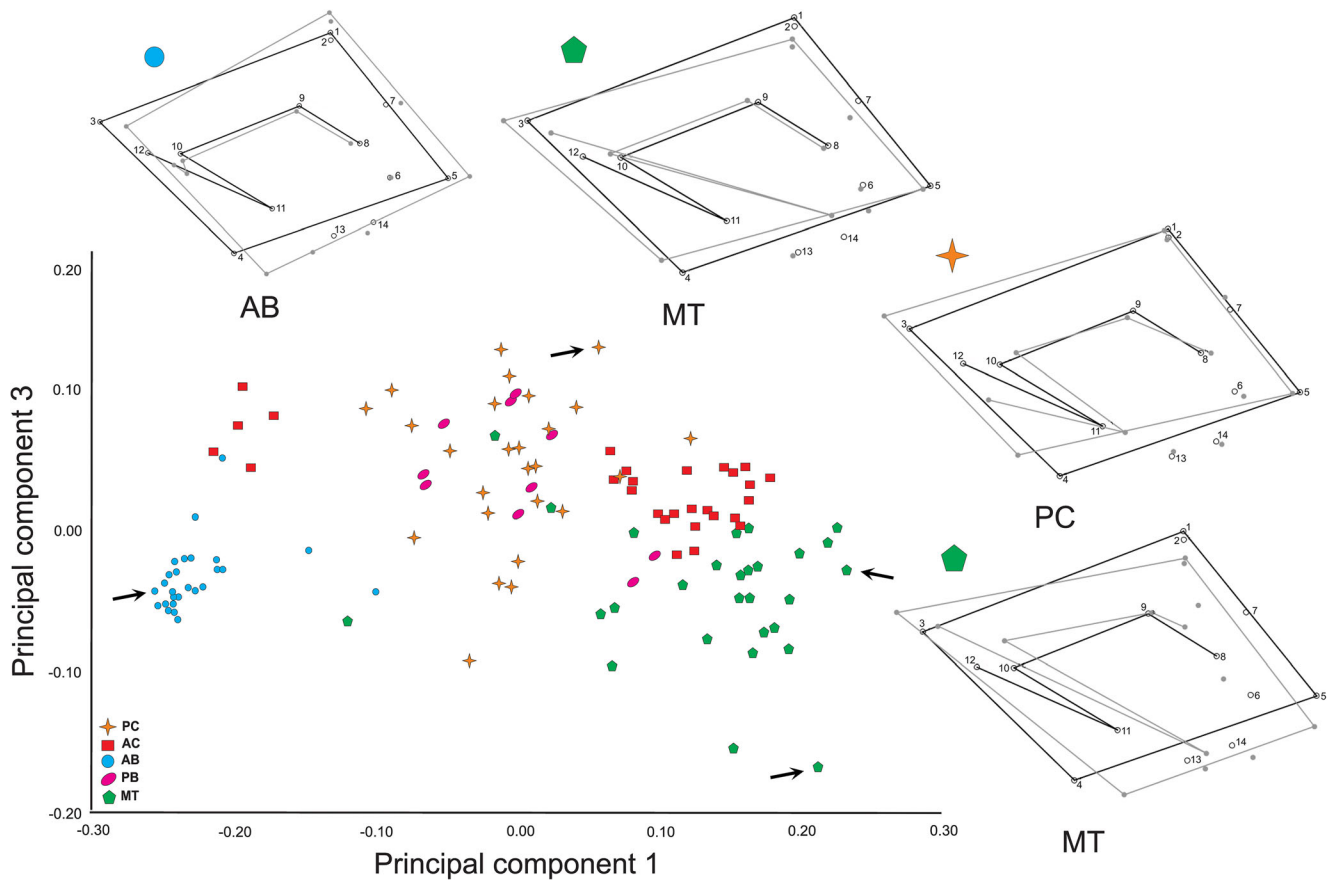
Fig. 5 Graphical representation of the first and third principal components axes including *Psammotreta brevifrons* in the analysis. The wireframes of four specimens (in gray) in extreme positions of the axes compared to the consensus shape (in black) are illustrated to show variation along the first and second principal components axes. The arrows indicate the specimens represented. AB, *Austromacoma biota*; PB, *Psammotreta brevifrons*; AC, *Austromacoma constricta*; PC, *Psammotreta cleryana*; MT, *Macoploma tenta*

2003; Piffer et al. 2011). Deposit feeders, oval shell species, and species which acquire a horizontal life position are common in Tellinidae. *Eurytellina lineata* (Turton, 1819), for example, has a striking similarity to *A. constricta* and *A. biota* and occupies the same type of dissipative or sheltered intertidal environment (Arruda et al. 2003). According to

Table 2 Differences in shape between the five Macominae species, pair-by-pair: Procrustes distance, Mahalanobis distance, the *T*-square statistic and associated parametric *P*-value, permutation test and associated bootstrap and parametric *P*-values AB *Austromacoma biota*, PB *Psammotreta brevifrons*, AC *Austromacoma constricta*, PC *Psammotreta cleryana*, MT *Macoploma tenta*

	Discriminant analysis				Permutation test		
	Procrustes d.	Mahalanobis d.	*T*-square	*P* value parametric	Goodall's *F*	*P* value bootstrap	*P* value parametric
AB vs PB	0.28444151	32.3184	8073.5510	<.0001	78.83	0.009	<.001
AB vs AC	0.31930514	11.6793	1838.9496	<.0001	85.62	0.009	<.001
AB vs PC	0.26035277	21.4999	6009.2084	<.0001	87.36	0.009	<.001
AB vs MT	0.37715069	18.3442	4536.6638	<.0001	136.39	0.009	<.001
PB vs AC	0.23742579	21.8883	3783.6361	<.0001	21.45	0.009	<.001
PB vs PC	0.08105115	5.1075	201.6410	0,0299	4.07	0.009	<.001
PB vs MT	0.17130641	7.9775	502.6027	0,0001	13.12	0.009	<.001
AC vs PC	0.20855242	22.1986	6643.3780	<.0001	30.41	0.009	<.001
AC vs MT	0.21091940	16.9793	4036.1665	<.0001	27.56	0.009	<.001
PC vs MT	0.17729486	8.1376	892.7427	<.0001	24.96	0.009	<.001

Table 3 Cross-validation matrix classification of discriminant function among the five Macominae species: *AB Austromacoma biota*, *PB Psammotreta brevifrons*, *AC Austromacoma constricta*, *PC Psammotreta cleryana*, *MT Macoploma tenta*

		Group 1				
Group 2		AB	PB	AC	PC	MT
	AB	X	100%	96.15%	100%	100%
	PB	100%	X	100%	72.73%	100%
	AC	100%	100%	X	100%	100%
	PC	100%	73.07%	100%	X	100%
	MT	100%	78.60%	100%	92.85%	X

Stanley (1970), the life position of *M. tenta* is similar to that of *A. biota* and *A. constricta*, lying on the left valve, but is slightly inclined, with the posterior region upwards. This position may explain the posterior flexure to the right seen in *M. tenta*, which is less prominent than in *A. biota* and *A. constricta*. There are no studies that demonstrate the position in sediment of *P. brevifrons* and *P. cleryana* under wild conditions, but their more elongated and streamlined shells, with a weak posterior flexure to the right, suggest they remain inclined, like *M. tenta* (Table 4).

Austromacoma biota differs from *A. constricta* in landmark 11, the intersection point of the pallial sinus with the pallial line, which is more anterior than in *A. constricta* (Fig. 4), a characteristic also supported by Arruda and Domaneschi (2005) and Piffer et al. (2011). This shows that the pallial sinus is only slightly detached from the pallial line in *A. biota* and very detached in *A. constricta*. It also demonstrates that, anatomically, the retracting muscles of the siphons in these two species are different. Hypothesizing that the siphon retracting musculature in *A. biota* is more robust and closer to the mantle margin than in *A. constricta*, its siphons can most likely be retracted more quickly than those of *A. constricta*. This rapid retraction is likely to result in more particles entering the mantle cavity, obstructing the gills. One finding that confirms that *A. biota* handles larger amounts of material in the mantle cavity than *A. constricta* is the presence of paired siphonal organs in *A. biota*, while *A. constricta* has only a single unilateral left siphonal organ (Piffer et al. 2011). The particles caught by the siphonal organs in *A. biota* are conveyed to the posterior extremity of the waste channel and eliminated as pseudofeces (Piffer et al. 2011).

The cruciform muscle, localized at the base of the siphonal internal apertures, connecting the ventral mantle lobes, characterizes species of Tellinoidea. The function of the cruciform muscle is still poorly understood, but it appears to have the function of anchoring the siphons during retraction and protraction (Yonge 1949) and also of working as a ventral pivot during the rocking movements involved in burrowing

Fig. 6 Cross-validation analysis between *Psammotreta brevifrons* (PB) (black line) and *Psammotreta cleryana* (PC) (gray line). **a** Lollipop graph showing the variation of each landmark comparing the analyzed species and **b** consensus wireframe graphs comparing the analyzed species
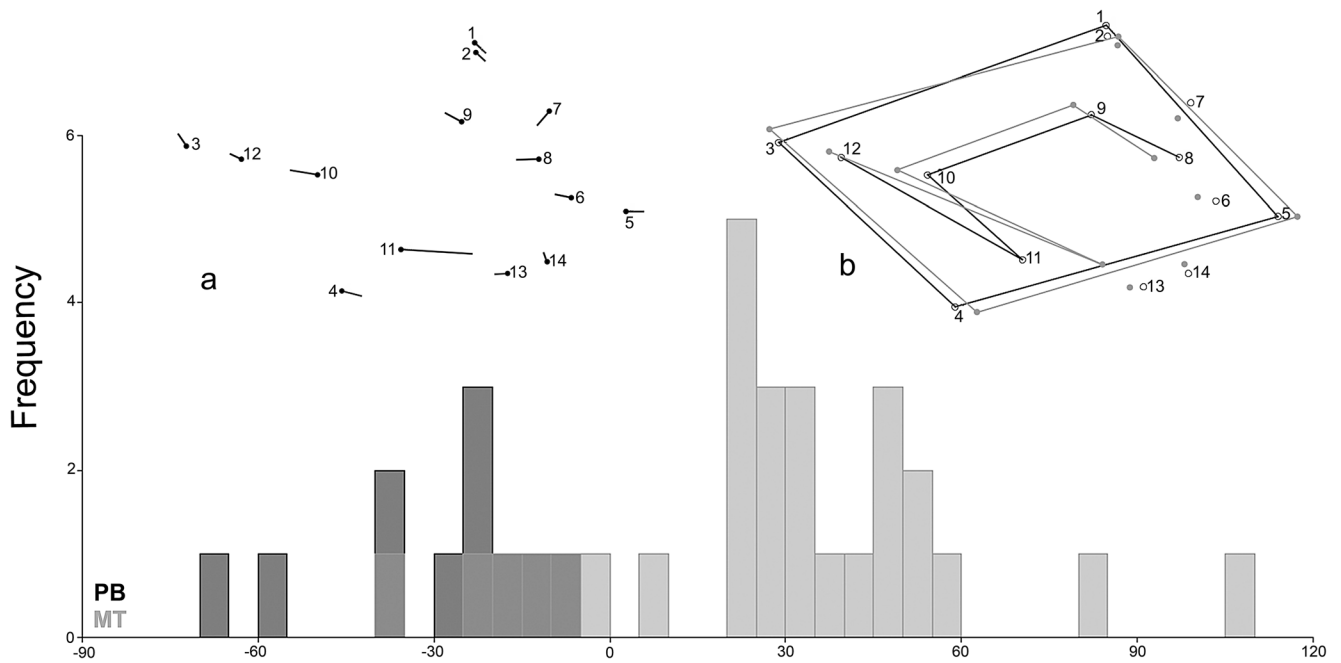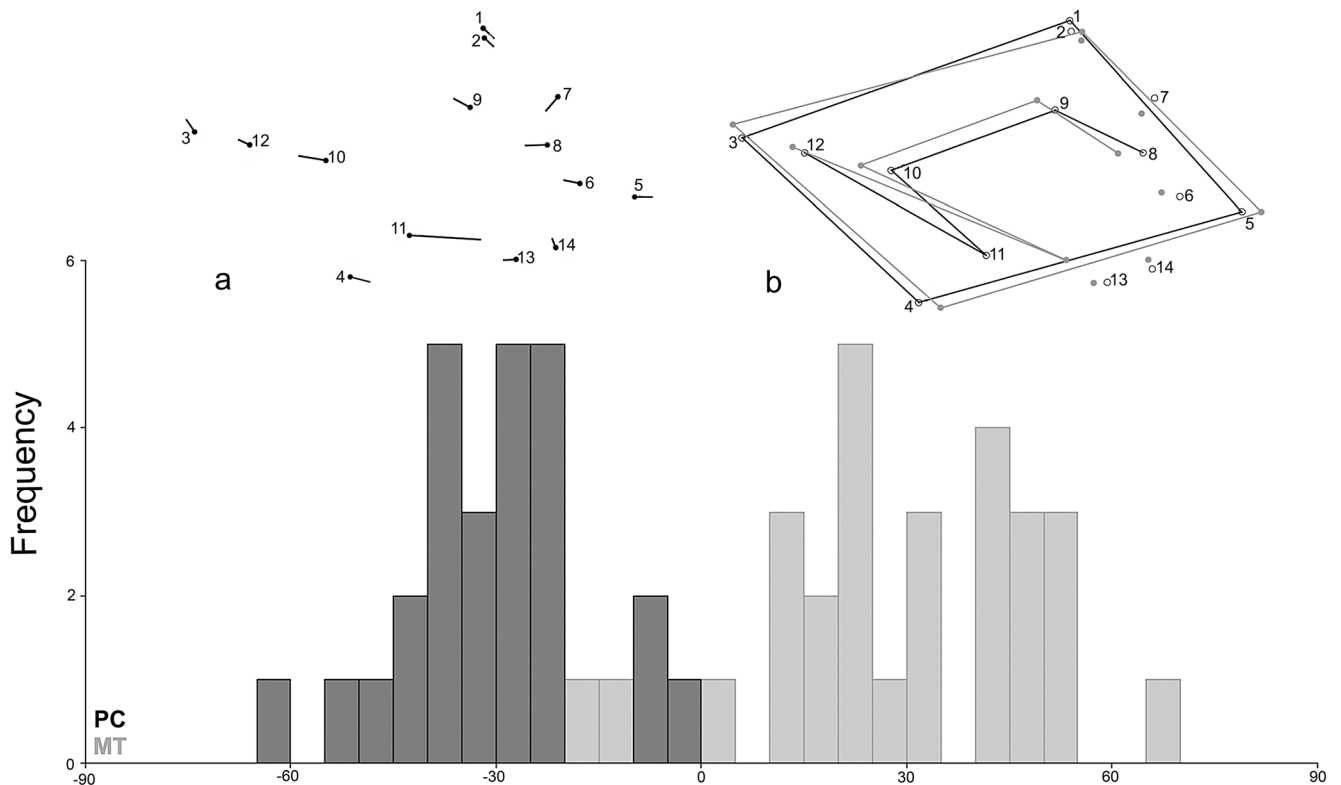
Fig. 7 Cross-validation analysis between *Psammotreta brevifrons* (PB) (black line) and *Macoploma tenta* (MT) (gray line). **a** Lollipop graph showing the variation of each landmark comparing the analyzed species and **b** consensus wireframe graphs comparing the analyzed species

(Watters 1993). The position of this muscle was represented in this study by landmarks 13 and 14. Generally, the species studied showed little variation in these landmarks, except for *A. biota*, in which the landmarks 13 and 14 are in a more anterior position than the consensus wireframe. In addition to the cruciform muscle, *A. biota* has an accessory adductor

Fig. 8 Cross-validation analysis between *Psammotreta cleryana* (PC) (black line) and *Macoploma tenta* (MT) (gray line). **a** Lollipop graph showing the variation of each landmark comparing the analyzed species and **b** consensus wireframe graphs comparing the analyzed species

Table 4 Shape and size characteristics associated with the life habits of the studied Macominae species

Species	Species Image	Species wireframe consensus (gray) compared to general consensus (black)	Length x height Minimum; maximum; mean	Habitat	Shell shape	Posterior flexure to right	Position on substrate	Rocking movements for burrowing
Austromacoma biota Arruda & Domaneschi, 2005			Min.: 4.3x3.4 Max.: 5.1x3.8 Mean: 4.54x3.53	Intertidal	Oval-trigonal	Strong		
Austromacoma constricta (Bruguière, 1792)			Min.: 4.0x3.2 Max.: 5.3x4.15 Mean: 4.71x3.73	Intertidal	Oval-trigonal	Strong		
Psammotreta brevifrons (Say, 1834 in Say 1830-1834)			Min.: 2.65x1.6 Max.: 2.9x1.9 Mean: 2.76x1.67	Shallow water up to 60m deep	Subelliptical elongated	Weak		
Psammotreta cleryana (d'Orbigny, 1846 in d'Orbigny, 1834-1847)			Min.: 2.85x1.65 Max.: 3.9x2.35 Mean: 3.42x2.01	Shallow water up to 40m deep	Subelliptical elongated	Weak		
Macoploma tenta (Say, 1834 in Say 1830-1834)			Min.: 1.45x0.8 Max.: 1.6x0.9 Mean: 1.56x0.84	Shallow water up to 130m deep	Subelliptical highly elongated	Moderate		

The size of the arrows in the last column compares the rocking movement between species: large and little movement

muscle, which to date has not been found in any other species of bivalve, located between the anterior and the posterior insertions of the cruciform muscle (Arruda and Domaneschi 2005). It is likely that this accessory adductor muscle interferes in the position of the cruciform muscle in *A. biota*. This muscle has the same function as the adductors (Piffer et al. 2011), but it is likely that it also reinforces the functions of the cruciform muscle, serving as a more robust anchorage during the rapid movement of the siphons.

In addition to the differences between *A. biota* and *A. constricta* described above, morphometric analysis highlighted the variation in the position of the anterior
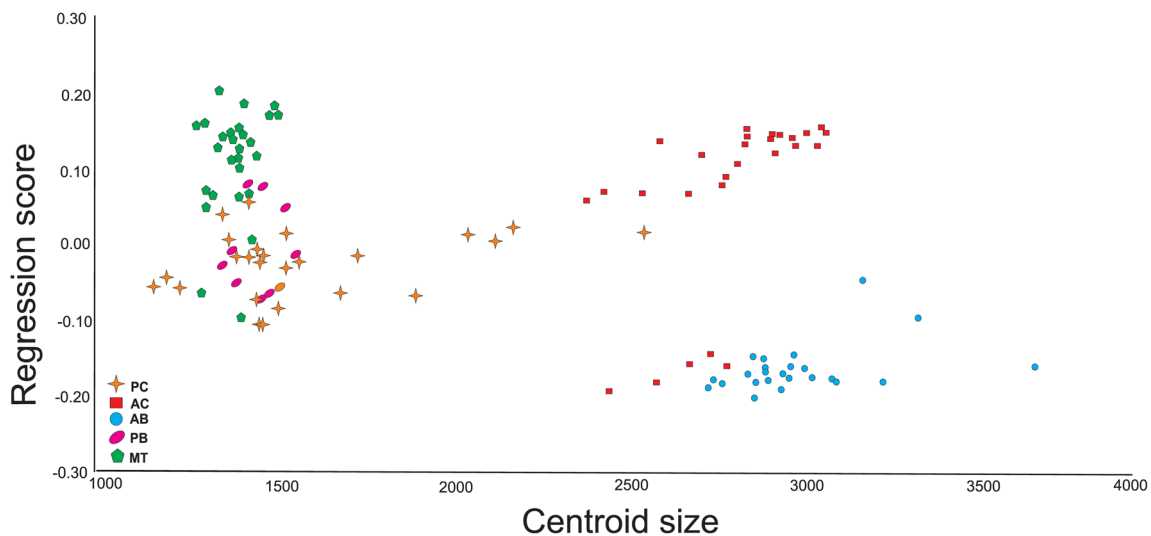

Fig. 9 Relationship between the regression score, representing the shape variation of the five studied species and the centroid size. AB, *Austromacoma biota*; PB, *Psammotreta brevifrons*; AC, *Austromacoma constricta*; PC, *Psammotreta cleryana*; MT, *Macoploma tenta*

adductor muscle scar, represented by landmark 12, which in *A. biota* is more dorsal than in *A. constricta*. This means that the anterior adductor muscle of *A. constricta* has a larger dorsoventral axis than the same muscle in *A. biota*.

Comparing the elongated group, *P. brevifrons*, *P. cleryana*, and *M. tenta*, the latter is that most differs (Fig. 6, 7, and 8), as its anterior adductor muscle is positioned more anteriorly, illustrated by landmark 12, and its specimens are longer and shorter than the others. Landmark 11 varies among the individuals of *M. tenta*, which explains the reason for the misidentification of some individuals during the analysis (see Figs. 4 and 5). This more elongated form of *M. tenta* suggests that its burrowing behavior differs from other species. The physiology of bivalve burrowing is well known, with a rocking movement occurring when the foot is anchored in the substratum and the contraction of the pedal retractor muscles (first the anterior and then the posterior) pulls the bivalve into the sediment (Stanley 1970). Stanley (1970) demonstrated that there is a relationship between the angle of rotation during the rocking movement and the degree of elongation, measured by the relationship between length and height (L/H), and that highly elongated species tend to use little or no rocking movement during burrowing, penetrating the substratum in an almost parallel direction to the long axis of the shell, while moderately elongated forms tend to use larger angles of rotation. *Macoploma tenta* exhibits little or no rocking movement during burrowing (Stanley 1970), while based on the external shape of the shells of *P. brevifrons* and *P. cleryana*, which are less elongated than *M. tenta*, we can assume that these species exhibit larger rocking movements, as do *A. biota* and *A. constricta* (Table 4). It is likely, however, that these species have even smaller rotation angles than highly rounded species, such as those of the Veneridae family.

In addition to the external shape of the shell and the position of the anterior adductor muscle scar, *M. tenta* differs from the other elongated species by the shape of its posterior adductor muscle scar, represented by landmarks 6 and 7, and that of the pallial sinus, represented by landmarks 8, 9, and 10. Landmarks 6 and 7 delimit the ventral and dorsal extremity of the posterior adductor muscle scar, respectively. The more dorsal position of landmark 6 and the more ventral position of landmark 7 demonstrate that the posterior adductor muscle of *M. tenta* has a smaller dorsoventral axis, which is more rounded than that of the other species. The more anterior position of landmarks 8, 9, and 10 demonstrates that *M. tenta* has a deeper pallial sinus.

Based on morphological similarity, *Psammotreta brevifrons* resembles *P. cleryana* (Tenório et al. 1986), supported by the results obtained in this study, and the occurrence of both species overlaps on the Brazilian coast (Rios 1970, 1974, 1985, 1994, 2009) and Western Atlantic coast (Huber 2015). Based on this analysis, *P. cleryana* should be considered a synonym of *P. brevifrons*. Huber (2015) has stated that the holotype of *P. cleryana* does not differ from *P. brevifrons* but also considered the latter to be variable along the Western Atlantic coast. Further detailed populational studies are therefore necessary to provide a better characterization of this species.

Despite the significant environmental effects suffered by shell morphology, and its disjointed characters, which often make taxonomic description abstract, detailed morphological analysis can be extremely useful in distinguishing bivalves. The results of the present study demonstrate that the geometric morphometric approach is especially useful when validating these characteristics of continuous variation and can provide important information for comparing the life habits of species. The external shape of the shell, the pallial sinus, and the adductor muscles proved to be efficient features for differentiating Macominae species.

Declarations

Conflict of interest The authors declare no competing interests.

Ethical approval No animal testing was performed during this study, and only fixed animals deposited in zoological collections were used.

Sampling and field studies The study does not contain sampling material or data from field studies.

Data Availability The datasets generated during the current study are available as supplementary material.

Author contribution EPA conceived and designed the research. TAM performed the morphometric analysis and prepared the figures for publication. EPA and TAM analyzed data and wrote the manuscript.

References

Adams DC, Rohlf FJ, Slice DE (2004) Geometric morphometrics: ten years of progress following the "revolution". Ital J Zool 71:5–16. https://doi.org/10.1080/11250000409356545

Anderson LC (2001) Temporal and geographic size trends in Neogene Corbulidae (Bivalvia) of tropical America: using environmental sensitivity to decipher causes of morphological trends. Paleogeogr Paleoclimatol Paleoecol 166:101–120. https://doi.org/10.1016/S0031-0182(00)00204-2

Anderson LC, Roopnarine PD (2005) Role of constraint and selection in the morphologic evolution of *Cariocorbula* (Mollusca: Corbulidae) from the Caribbean Neogene. Palaeontol Electron 8 http://palaeo-electronica.org/paleo/2005_2/mollusca/issue2_05.htm. Accessed 22 February 2016

Arruda EP, Domaneschi O (2005) New species of *Macoma* (Bivalvia: Tellinoidea: Tellinidae) from southeastern of Brazil, and with description of gross anatomy. Zootaxa 1012:13–22. https://doi.org/10.11646/zootaxa.1012.1.2

Arruda EP, Domaneschi O, Amaral ACZ (2003) Mollusc feeding guilds on Sandy beaches in São Paulo State, Brazil. Mar Biol 143:691–701. https://doi.org/10.1007/s00227-003-1103-y

Bookstein FL (1991) Morphometric tools for landmark data. Geometry and Biology. Cambridge University Press, Cambridge

Bruguière JG (1792) Catalogue des coquilles envoyées de Cayenne, à la Société d'histoire naturelle de Paris, par M. Le Blond. *Actes de la Société d'Histoire Naturelle de Paris* 1:126–129

Coan EV, Valentich-Scott P (2012) Bivalve seashells of tropical West America: marine bivalve mollusks from Baja California to Northern Perú. Santa Barbara Museum of Natural History, Santa Barbara

Dall WH (1900) Synopsis of the family Tellinidae and of the North American species. Proc US Nat Museum 23(1210):285–326. https://www.biodiversitylibrary.org/part/26632. Accessed 20 Mar 2021

Drake AG, Klingenberg CP (2008) The pace of morphological change: historical transformation of skull shape in St Bernard dogs. Proc Roy Soc 275:71–76. https://doi.org/10.1098/rspb.2007.1169

Dryden, IL (2019) Shapes: statistical shape analysis. R package version 1.2.5. https://CRAN.R-project.org/package=shapes. Accessed 27 January 2021

Hammer Ø, Harper DAT, Ryan PD (2001) PAST: paleontological statistics software package for education and data analysis. Palaeontol Electron 4(1) 9pp http://palaeo-electronica.org/2001_1/past/issue1_01.htm. Accessed 27 January 2021

Huber M (2015) Compendium of Bivalves 2. Harxheim, Germany. ConchBooks, 907pp

Inoue K, McQueen AL, Harris JL, Berg DJ (2014) Molecular phylogenetics and morphological variation reveal recent speciation in freshwater mussels of the genera Arcidens and Arkansia (Bivalvia: Unionidae). Biol J Linn Soc 112:535–545. https://doi.org/10.1111/bij.12282

Jensen RJ (2003) The conundrum of morphometrics. Taxon 52:663–671

Klingenberg CP (2011) MORPHOJ: an integrated software package for geometric morphometrics. Mol Ecol Resour 11:353–357. https://doi.org/10.1111/j.755-0998.2010.02924.x

Klingenberg CP (2013) Visualizations in geometric morphometrics: how to read and how to make graphs showing shape changes. Hystrix 24(1):15–24. https://doi.org/10.4404/hystrix-24.1-7691

Klingenberg CP (2016) Size, shape, and form: concepts of allometry in geometric morphometrics. Dev Genes Evol 226:113–137. https://doi.org/10.1007/s00427-016-0539-2

Kosnik MA, Jablonski D, Lockwood R, Novack-Gottshall PM (2006) Quantifying molluscan body size in evolutionary and ecological analyses: maximizing the return on data-collection efforts. Palaios 21:588–597. https://doi.org/10.2110/palo.2006.p06-012r

Marko PB, Jackson JBC (2001) Patterns of morphological diversity among and within Arcid bivalve species pairs separated by the Isthmus of Panama. J Paleontol 75(3):590–606. https://doi.org/10.1666/0022-3360(2001)075<0590:POMDAA>2.0.CO;2

Marquez, F, Trivellini, MM, Van der Molen, S (2017) Use of shell shape variation as assessment tool in the southernmost razor clam fishery. Fish Res 186:216–222. https://doi.org/10.1016/j.fishres.2016.08.027

Monnet C, Klug C, De Baets K (2009) Evolutionary patterns of Ammonoids: phenotypic trends, convergence, and parallel evolution. In: Klug C, Korn D, De Baets K, Kruta I, Mapes R (eds) Ammonoid Paleobiology: From macroevolution to paleogeography. Top Geobiol, vol 44. Springer, Dordrecht. https://doi.org/10.1007/978-94-017-9633-0_5

Monteiro LR, Reis SF (1999) Princípios de Morfometria Geométrica. Editora Holos

Moraes DA (2003) A Morfometria Geométrica e a "Revolução na Morfometria" Localizando e visualizando mudanças na forma dos organismos. Bioletim 3. São Paulo, SP

Mikkelsen PM, Bieler R (2008) Seashells of Southern Florida: living marine mollusks of the Florida Keys and adjacent regions: bivalves. Princeton University Press

Narchi W (2003) The relationship between the unilateral siphonal organ and labial palps of *Macoma constricta* (Bruguière, 1792) (Bivalvia, Tellinidae). J Molluscan Stud 69:359–363. https://doi.org/10.1093/mollus/69.4.359

Orbigny, AD d' (1834-1847). Voyage dans l'Amérique méridionale [...] exécuté pendant les années 1826, 1827, 1828, 1829, 1830, 1831, 1832 et 1833. Tome 5(3) Mollusques. pp. i–xliii, 1–758, 85 plates

Piffer PR, Arruda EP, Passos FD (2011) The biology and functional morphology of *Macoma biota* (Bivalvia: Tellinidae: Macominae). Zoologia 28(3):321–333. https://doi.org/10.1590/S1984-46702011000300006

Reis SF (1998) Morfometria e Estatística Multivariada em Biologia Evolutiva. Rev Brasil Zool 5(4):571–580. https://doi.org/10.1590/S0101-81751988000400005

Rios EC (1970) Seashells of Brazil. Fundação Universidade do Rio Grande, Museu Oceanográfico, Rio Grande

Rios EC (1974) Seashells of Brazil. Fundação Universidade do Rio Grande, Museu Oceanográfico, Rio Grande

Rios EC (1985) Seashells of Brazil. Fundação Universidade do Rio Grande, Museu Oceanográfico, Rio Grande

Rios EC (1994) Seashells of Brazil. Fundação Universidade do Rio Grande, Museu Oceanográfico, Rio Grande

Rios EC (2009) Coastal Brazilian seashells. Fundação Universidade do Rio Grande, Museu Oceanográfico, Rio Grande

Rocha VP (2011) Morfometria e anatomia de Arcídeos (Mollusca, Bivalvia) da Costa Norte – Nordeste do Brasil. Dissertation, Universidade Federal do Ceará, Fortaleza, CE.

Rohlf FJ (1990) Morphometrics. Annu Rev Ecol Syst 21:299–316. https://doi.org/10.1146/annurev.es.21.110190.001503

Rohlf FJ (2000a) Geometric morphometrics and phylogeny. Department of Ecology and Evolution, State University of New York at Stony Brook, Stony Brook

Rohlf FJ (2000b) Statistical power comparisons among alternative morphometric methods. Am J Phys Anthropol 111:463–478. https://doi.org/10.1002/(SICI)1096-8644(200004)111:4<463::AID-AJPA3>3.0.CO;2-B

Rohlf FJ (2000c) On the use of shape spaces to compare morphometric methods. Hystrix 11:9–25. https://doi.org/10.4404/hystrix-11.1-4134

Rohlf FJ, Marcus LF (1993) A revolution in morphometrics. Tree 8(4): 129–132

Rohlf FJ, Adams DC, Slice DE (2004) Geometric Morphometrics: ten years of progress following the "revolution". Ital J Zool 71:5–16. https://doi.org/10.1080/11250000409356545

Rufino MM, Gaspar MB, Pereira AM, Vasconcelos P (2006) Use of shape to distinguish Chamelea gallina and Chamelea striatula (Bivalvia: Veneridae): linear and geometric morphometric methods. J Morphol 267:1433–1440. https://doi.org/10.1002/jmor.10489

Say T. (1830–1834). American Conchology or descriptions of the shells of North America. Illustrated by colored figures from original drawings executed from nature. School Press, New Harmony, Indiana. Part 1 (1830a); Part 2 (April 1831a); Part 3 (September 1831a); Part 4 (March 1832); Part 5 (August 1832); Part 6 (April 1834); Part 7 (1834? edited by TA Conrad).

Sheets HD, Covino KM, Panasiewicz JM, Morris SR (2006) Comparison of geometric outline methods in the discrimination of age-related differences in feather shape. Front Zool 3:1–12. https://doi.org/10.1186/1742-9994-3-15

Simone LRL, Wilkinson S (2008) Comparative morphological study of some Tellinidae from Thailand (Bivalvia: Tellinoidea). Raffles Bull Zool 18(Supplement):151–190

Stanley SM (1970) Relation of shell for to life habits of the Bivalvia (Mollusca). The Geological Society of America, Inc. Memoir 125.

Tenório DO, Mello RLS, Silva OC (1986) O Gênero Macoma Leach, 1819 (Bivalvia Tellinidae) na plataforma continental Brasileira. Cadernos Ômega da Universidade Federal Rural de Pernambuco, Série Ciências Aquáticas, 2: 7–39.

Viscosi V, Cardini A (2011) Leaf morphology, taxonomy and geometric morphometrics: a simplified protocol for beginners. PLoS ONE 6(10):e25630. https://doi.org/10.1371/journal.pone.0025630

Vuolo I, Gianolla D, Cerone EP, Seu D (2011) Variation in shell morphology in the fossil freshwater gastropod Tanousia subovata (SETTEPASSI 1965) from the Mercure Basin (Middle Pleistocene, southern Italy): distinct taxa or ecophenotypic variation? (Gastropoda Prosobranchia: Hydrobiidae). Archiv Molluskenkunde: Int J Malacol 140:19–28. https://doi.org/10.1127/arch.moll/1869-0963/140/019-028

Watters GT (1993) Some aspects of the functional morphology of the shell of infaunal bivalves (Mollusca). Malacologia 35:315–342

Zelditch ML, Swiderski DL, Sheets HD, Fink WL (2004) Geometric morphometric for biologists: a primer. Elsevier, New York

Yonge CM (1949) On the structure and adaptations of the Tellinacea, deposit-feeding Eulamellibranchia. Philos Trans Roy Soc Lond Ser B 324:29–76